Supporting Information

Nanodiscs for INPHARMA NMR Characterization of GPCRs: Ligand Binding to the Human A2A Adenosine Receptor

Kai Fredriksson[+],* Philip Lottmann, Sonja Hinz, Iounut Onila, Aliaksei Shymanets, Christian Harteneck, Christa E. Müller, Christian Griesinger, and Thomas E. Exner*

anie_201612547_sm_miscellaneous_information.pdf

Supporting Information

Table of Contents

Materials and Methods

Biochemistry Methods

Sf9 expression of A2AR

DNA encoding a wild-type A_{2A} adenosine receptor (ADORA2A or $A_{2A}R$) insert ready in Bac-to-Bac vector was ordered from GenScript. The plasmid contained a C-terminal His_6-tag and before that a TEV-cleavage site. Recombinant protein was expressed in Sf9 insect cells as detailed in Invitrogen's Bac-to-Bac Baculovirus Expression System protocol. Sf9 cells were infected when the cell density was $1,5 \times 10^6$ and expressed for 48 hours. After expression cells were collected by centrifugation at 800 x g for 15 minutes and washed twice with PBS (phosphate-buffered saline), without Ca^{2+} and Mg^{2+}, pH 7.4 (PAA Laboratories GmbH). Cells were broken using nitrogen cavitation; 40 bar and 30 min. Then cells were collected by ultracentrifugation at 100 000 x g for 1 h, pellets were collected and stored at -80 ^{o}C for further use.

Protein purification

For nanodiscs, the pellet was resuspended in 25 mM phosphate buffer, 10 % glycerol, 100 mM NaCl and 0.1 mM Ethylenediaminetetraacetic acid (EDTA) with one protease pill in 5 g of cell pellet (Roche). 1% of *n*-dodecyl-β-D-maltopyranoside (DDM) and 0.2 % of Cholesteryl hemisuccinate (CHS) was added and then incubated in a vertical shaker for 1 h. Then, NaCl was added for a final concentration of 500 mM. The prepared sample was centrifuged at 100 000 x g for 30 min and the supernatant was subsequently collected.

For protein purification we used Talon Metal Affinity Resin. First 1 to 1.5 ml of well mixed resin were pipetted into a container which can hold ten to twenty times the volume of the resin. The resin was centrifuged down at 700 x g for 2 min. The supernatant was disposed of and resin were washed with ten to twenty volumes of washing buffer consisting of 25 mM sodium phosphate, pH 7.5, 10 % (w/v) glycerol, 500 mM NaCl, 0.1 % DDM. After a few minutes of gentle shaking the resin was centrifuged down again at 700 x g for 2 min. The protein supernatant from ultracentrifugation was added onto the resin and the mixture left in a cold room at +4° C in a vertical shaker for 20 min, then the resin was again centrifuged down at 700 x g for 5 min and washed once with washing buffer for 10 min at +4° C and centrifuged again at 700 x g for 5 min. The resin was moved to a gravitation column and allowed to settle down, washed in a three- to five-fold volume of washing buffer that contained 20 mM imidazole. Elution was performed directly into 1.5 ml Eppendorf tubes using washing buffer containing 150 mM imidazole. The samples were flash freeze and stored at -80° C for further use.

Nanodisc preparation

Two different kind of Membrane Scaffold Protein 1D1 (MSP1D1) were prepared one where the His-tag was removed using the TEV-cleavage site and another one, where no His-tag was attached. Both variants were expressed in E. coli using LB medium. Bacteria were incubated at +37° C and shaken at 180 rpm until an OD 600 of 0.8 was reached. Expression was induced by addition of 1 M Isopropyl-β-D thiogalactopyranosid (IPTG) to a final concentration of 1 mM. Cells were harvested by centrifugation for 30 minutes and 4000 rpm at +4° C, washed once using PBS buffer, centrifuged for 15 min at 4000 rpm at +4° C and stored at -20° C for future use. Cells were then resuspended using MSP1D1 lysis buffer (40 mM

Tris/HCl pH 8.0, 300 mM NaCl, 1 % Triton X-100, 4 mM sodium azide), 4 ml/g of cells, spatula tip of $MgCl_2$ and DNAse I and one protease pill (Roche) in 5 g of cells. Cells were then lysed by sonication. The sonicated cells were centrifuged for 1 hour at 100 000 x g and the supernatant was filtered with a 0.2 μm syringe filter and then loaded to a Ni^{2+}-sepharose column 2 ml/min, equilibrated by MSP lysis buffer. After loading, the column was washed using 4 bed volumes of MSP lysis buffer then: 1) 40 mM Tris/HCl, pH 8.0, 300 mM NaCl, 50 mM sodium cholate; 2) 40 mM Tris/HCl, pH 8.0, 300 mM NaCl; 3) 40 mM Tris/HCl, pH 8.0, 300 mM NaCl, 50 mM imidazole. Protein was eluted using MSP elution buffer (40 mM Tris/HCl, pH 8.0, 300 mM NaCl, 300 mM imidazole, 4mM sodium azide) and fractions containing protein were collected. At this point MSP1D1 without His-tag was prepared as follows: after determination of MSP1D1 concentration 1 mg of TEV-protease was added to every 5 mg of protein and was subjected to dialysis in MSP-His-tag cleavage buffer (50 mM Tris/HCl, pH 8.0, 0.5 mM EDTA, 1mM DTT) in 6 kDa molecular weight cut-off (MWCO) membrane at room temperature overnight. On the next day the dialysis was continued against 20 mM Tris/HCl, pH 8.0, 150 mM NaCl, at +4° C overnight. After this sodium cholate was added to a final concentration of 50 mM. The Ni^{2+}-sepharose loaded column was equilibrated using MSP purification buffer (20 mM Tris/HCl, pH 8.0, 150 mM NaCl, 50 mM sodium cholate). MSP was loaded to the column and eluted fractions were collected and finally dialyzed against nanodisc buffer (20 mM Tris/HCl, pH 7.4, 100 mM NaCl). The concentration of MSP1D1 was measured and we prepared 1 mg/ml vials of 1 ml volume, flash froze them using liquid nitrogen and stored them at -80° C. To prepare MSP1D1 with His-tag, the expressed protein was simply dialyzed once after the first Ni^{2+} Sepharose loaded column against nanodisc buffer, measured and stored after that.

For the preparation of loaded nanodiscs, MSP1D1 scaffold protein and 1-palmitoyl-2-oleoyl-sn-glycero-3-phosphocholine (POPC) lipids from Avanti Polar Lipids were used. Nanodiscs with adenosine $A_{2A}R$ were prepared using molar ratios 1:25:750, $A_{2A}R$, MSP1D1 and POPC respectively. First, samples were incubated on ice for one hour using 20 mM Tris/HCl, pH 7.4, 100 mM sodium cholate, 10 mg/ml of lipids and 0.1 % DDM. Washed and swelled Bio Beads (Biorad) were added 0.5 g per ml of sample and incubated for 90 min at +4° C in a vertical shaker. Samples were then filtered using 0.45 μm syringe filter and loaded on a 10/300 sepharose column and eluted in 1 ml fractions using the SEC buffer.

Loaded discs were purified using Talon Metal Affinity Resin using 25 mM phosphate buffer with 150 mM NaCl. Eluted by 250 mM imidazole, the sample was desalted and the buffer was exchanged using PD Mini Trap G-25 (GE Healthcare) gel filtration columns. G25 columns were first equilibrated with twice the column volume using 25 mM phosphate buffer pH 7.0 and 150 mM NaCl in 100 % deuterium oxide. 0.5 ml of sample was introduced into the column and then eluted using 1 ml of equilibrating buffer. In the end the sample was concentrated up to 4 μM using Amicon Ultra-0.5 ml, 30 kDa viacons, first washed with 0.1 M NaOH and with 25 mM phosphate buffer pH 7.0 and 150 mM NaCl in 100 % deuterium oxide before use.

For the negative control we prepared empty discs without $A_{2A}R$. The protocol was identical to the protocol to prepare loaded nanodiscs expect for a change of the MSP:POPC stoichiometry. For loaded nanodiscs, the ratio was 1:30, while for empty ones it was 1:35. Empty discs were also purified to remove free lipids. The buffer was exchanged and the discs were concentrated to the same final concentration as in the case of the loaded ones. Concentrations of final samples were adjusted by absorbance of 280 nm (A_{280}) using extinction coefficients as follows; for $A_{2A}R$ 57255 and for MSP1D1 18450, assuming that there is one receptor per one nanodisc and one disc contains two MSP proteins.
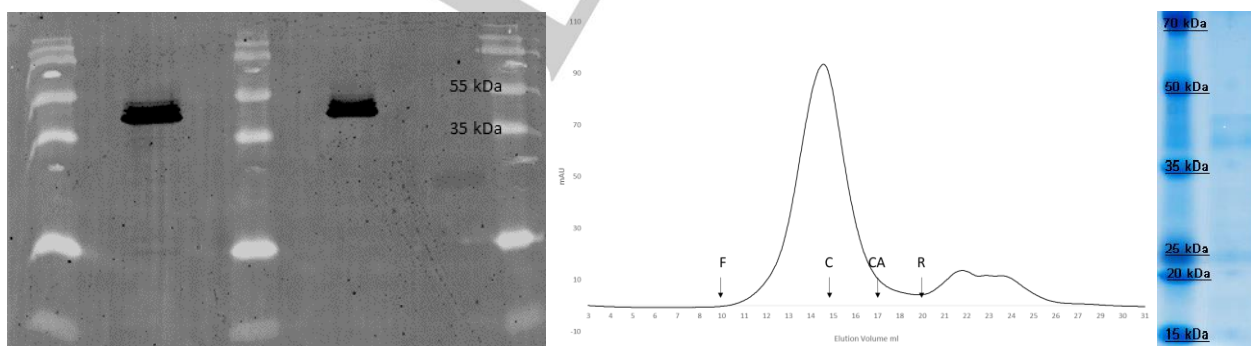

Figure S1. On the left; Western-blot picture of $A_{2A}R$ in sf9 insect cell extract, detected using anti-His antibody. Middle; size exclusion chromatography elution curve of $A_{2A}R$ incorporated with MSP1D1 nanodiscs of Superdex 200 increase 10/30 GL column, where calibration of column has been made using standart marker proteins as follows; F) Ferritin, 440 kDa and 10,97 ml, C) Conalbumin, 75 kDa and 14,90 ml, CA) Carbonic Anhydrase 29 kDa and 16,83 ml, R) Ribonuclease A 13,7 kDa and 19,53 ml. On the right; SDS-PAGE gel of 4 μM NMR sample; $A_{2A}R$ Adenosine is visible around 46 kDa, MSP1D1 below 25 kDa. Due low concentration, the receptor is not visible in SDS-PAGE gel of SEC fractions.

NMR Methods

Sample preparation

Stock solutions of all ligands were prepared in DMSO-d_6 as solvent at a concentration of 32 mM, except for the stock solution of XAC which had a concentration of 7 mM due to a limited solubility. The internal standard and chemical shift reference TSPA-d_6 was dissolved in D_2O at a concentration of 2 mM. These stock solutions were pipetted to a nanodisc solution previously diluted by buffer. The final concentration of the nanodiscs after the addition of the ligands was 4 μM. In all experiments not involving SYN115, the ligand concentration of caffeine, PQA and ZMA was 300 μM. In experiments with SYN115, the concentration was 200 μM for PQA, ZMA and SYN. Later, XAC was added to the samples up to a total concentration of 50 μM. The concentration of TSPA was in all experiments 20 μM. All samples were filled into 3 mm NMR-tubes with a total sample volume of 120 μL**.**

NMR Experiments

All NMR experiments were conducted at 700 MHz, either on a Bruker AVANCE III spectrometer equipped with an Oxford magnet and a Bruker CryoProbe Prodigy, or on a Bruker AVANCE I spectrometer equipped with a Bruker US magnet and a Bruker CryoProbe. All measurements were conducted at 298 K.

One-dimensional proton spectra were recorded with a relaxation time of 2 s. The residual water signal was suppressed by presaturation. The signal was acquired for 487 ms with 8192 data points.

The STD-experiments were set up with a relaxation time of 2 s and a selective saturation time of 3 s. For this purpose, a cascade of Gaussian pulses with a length of 20 ms was applied. The on-resonance frequency was set to -1 ppm and the off-resonance frequency to 50 ppm. A 3-9-19 watergate pulse scheme was used for water suppression. The FID was recorded with 4096 data points and a length of 243 ms. The presence or absence of the TSPA-d6 signal and the signal of DMSO-d_6 in the STD spectra was used as a control of the experimental setup. In all recorded STD experiments with nanodiscs neither of the mentioned substances gave rise to a STD signal.

For the INPHARMA measurements, a NOESY experiment with water presaturation was used. 4096 data points in the direct dimension and 600 in the indirect dimension were acquired, which corresponds to an acquisition time of 243.3 ms and 35.6 ms, respectively. The relaxation time was 2s and a mixing time of 300 ms was measured in all experiments.

Spectral Analysis

The chemical shift in all spectra was referenced to the residual protons of DMSO-d_6, which was added to the samples via the stock solutions of the ligands. The chemical shift was set to 2.70 ppm. The methyl signal of internal standard TSPA-d_6 showed in some samples minor chemical shift changes, specially, when the free lipid concentration was high. The chemical shifts of all ligands is summarized in table S1.

Table S1. Chemical shift assignment of the studied ligands.

Caffeine		PQA		SYN		ZMA		XAC	
Resonance	C. S. [ppm]	Resonance	C. S. [ppm]	Resonance	C. S. [ppm]	Resonance	C. S. [ppm]	Resonance	C. S. [ppm]
1	7.91	1	2.02	1	1.32	1	7.76	1	3.64
2	3.97	2	3.72	2	1.72	2	6.70	2	3.22
3	3.37	3	7.50	3	3.53	3	7.20	3	4.74*
4	3.55	4	7.39	4	3.80	4	3.63	4	7.14
		5	7.39	5	3.20	5	2.87	5	7.91
		6	7.62	6	3.99	6	7.21	6	3.93
				7	7.07	7	6.83	7	1.65
				8	3.99			8	0.95

											9	4.08
											10	1.81
											11	0.98

*based on the cross peaks in the recorded NOESY experiments at XAC concentrations above 200 µM

STD experiments and results

In order to compare the STD experiments, all signals of the ligands without overlap or artifacts were integrated and normalized to the signal intensities in the off resonance spectra. In the next step, the experimental values of the three samples - loaded discs without XAC (ST2), empty discs without XAC (ST1) and loaded discs with XAC (ST3) - , were compared. The normalized integrals of the sample with loaded discs and without XAC (ST2) were defined as 100 %. With this, the values for the other samples were calculated. We expected the following results for our STD measurements:

Table S2. Comparison of the measured STD intensities between the three samples: ST1 - loaded discs without XAC, ST2 - empty discs without XAC, ST3 - loaded discs with XAC. The sample with loaded discs and without XAC was used as reference.

Relative intensity in %	Caffeine - 1	Caffeine - 2	Caffeine - 3	PQA – 1	PQA - 3	PQA - 4 & 5	PQA – 6	ZMA – 1	ZMA – 2	ZMA - 3 & 6	ZMA – 5	ZMA – 7	Average:	Caffeine	PQA	ZMA
Reference Loaded discs w/o XAC	100	100	100	100	100	100	100	100	100	100	100	100		100	100	100
Empty discs w/o XAC	8	37	33	158	94	97	110	105	110	97	104	95		26	115	102
Loaded discs w/ XAC	120	117	82	75	89	86	87	85	78	80	69	86		106	84	80

Neither with empty nanodiscs (ST1) nor with loaded discs in the presence of XAC (ST3) STD signals should be observable for CAF, PQA, and ZMA due to the lack of a receptor and an accessible binding pocket, respectively. Opposite to our expectations, for all three ligands, STD signals were observed in both cases, although none were observed in buffer alone without nanodiscs. Therefore unspecific interactions between the scaffold protein and/or the lipids and the ligands must take place. Nevertheless, an accessible $A_{2A}R$ binding site (ST2) should add to these measured unspecific STD signals. Yet, out of the three ligands, only CAF showed four times stronger STD signals. In contrast, the presence of XAC (ST3) had no effect on the STD signals of CAF, but the signals of PQA and ZMA were reduced by approximately 20%. Based on these inconclusive findings, we discarded the STD experiments in the analysis of our system.

Data preparation for the SpInpharma calculations

The INPHARMA data was prepared in the following steps: Based on the assignment (table S 1) all cross and diagonal peaks were assigned and integrated.[1] All ligands had in all samples cross peaks which had the same sign as the diagonal peaks. This suggests an interaction between the ligands and the unloaded nanodiscs. In a consecutive step, the signals had to be normalized in order to compensate non-equilibrium conditions due to limited relaxation delays between scans and sensitivity changes between different samples and titration steps. For this purpose, the integral values were divided by the overall magnetization of each resonance, which corresponds to the sum of all peaks with the same frequency in the indirect dimension (F1).

This measure presents a few difficulties. Some peaks were overlapping with each other or impurities. Two of these are the peaks off resonance 3 and 6 of ZMA around 7.20 ppm and 7.21 ppm, respectively. In the direct dimension, both are overlapping but still distinguishable (Figure S1). Therefore the volumes had to be approximated based on the two integration areas (Figure S1 A and B). The area around 7.21(A) is one half of the doublet of resonance 6. Therefore it was

multiplied by two, in order to obtain the full integral of resonance 6.Accordingly, the integral around 7.21 (A) was subtracted from the integral around 7.20 ppm (B) to obtain the integral of resonance 3.
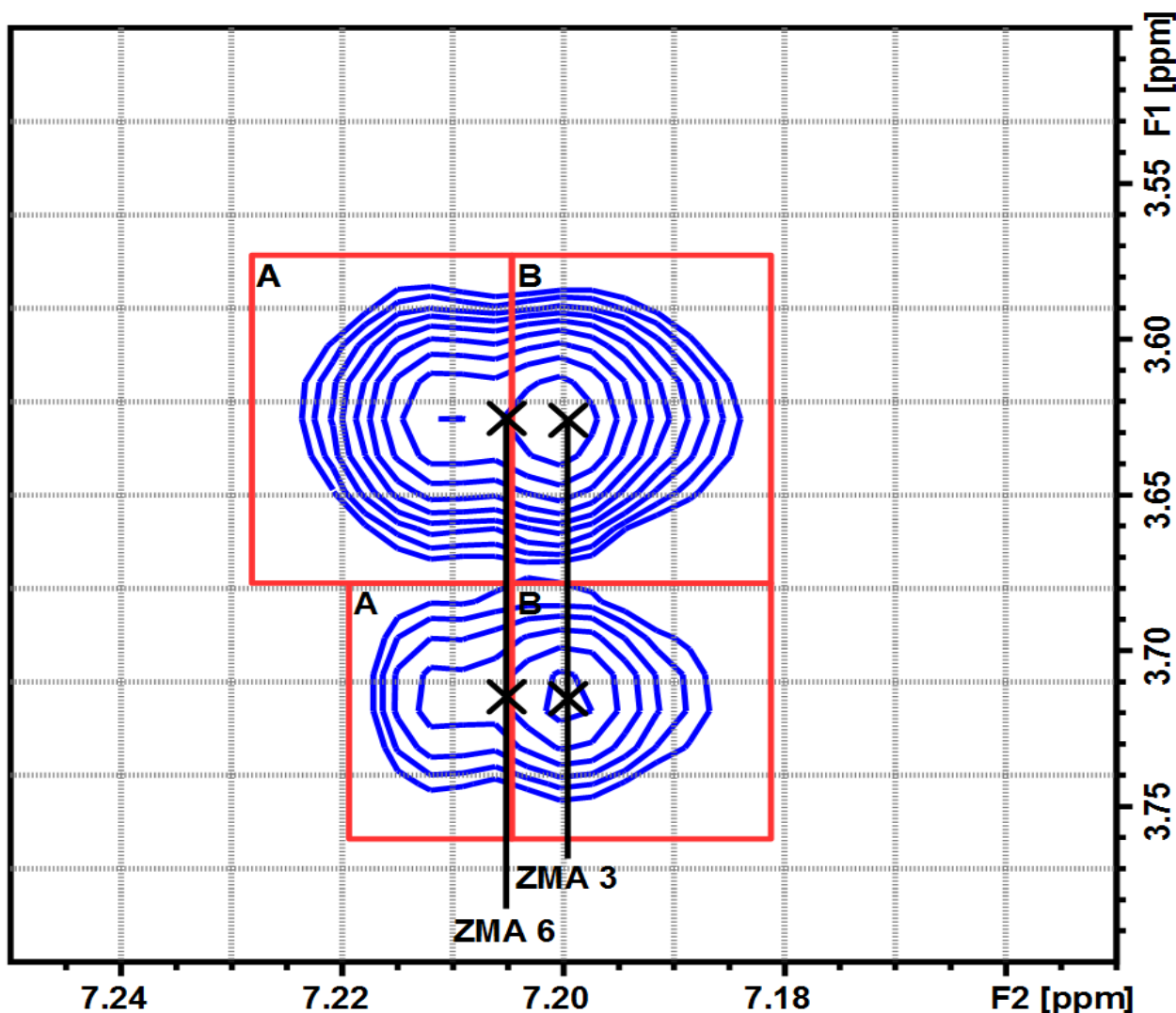

Figure S2: Exemplary section of a NOESY spectrum of ZMA. The peaks of resonances 3 and 6 are overlapping with a chemical shift of 7.200 ppm and 7.205 ppm, respectively. Resonance 6 is a doublet with its peaks at 7.200 and 7.210 ppm. A and B are the integration areas which were used to calculate the separated integrals of resonance 3 and 6.

In the indirect dimension, both resonances cannot be distinguished. Therefore, the overall integral of both was taken and split relative to the intensity ratios of the corresponding signals on the other half of the diagonal. In case of the diagonal peak, the proton ration of 2:1 was used to divide the integral.

Furthermore, the diagonal peaks of resonances 2 of PQA and 4 of ZMA are overlapping with signals from some impurities in the sample solution. This made it impossible to calculate the overall magnetization for these resonances. Hence, it was necessary to calculate the average of the overall magnetization per proton for each ligand based on the other resonances. These values were used to extrapolate the overall magnetization of these two resonances.

In a next step, the difference of the normalized signals between the samples a) with (ST2) and without XAC (ST3) and b) with (ST2) and without (ST1) $A_{2A}R$ was taken in order to remove contributions which are not related to the binding pocket. For this procedure to work, some corrections had to be made. Due to noise and low signal intensities, some integrals were negative and were therefore set to 0. Another effect of taking the difference between two spectra was that the diagonal peaks canceled each other out or became even negative. For the SPINPHARMA software, it was necessary to replace these values since the software requires normalized integrals. The sum of all normalized integrals (cross and diagonal peaks) of one resonance in the F1 dimension should equal 1, which is not true after the subtraction of the signals. Therefore, all differences of the normalized cross peaks in the indirect dimension were summed up and subtracted from 1, in order to obtain the volume of the diagonal peak.

In a last step, the spectrum was reflected at the diagonal (F1 = F2). This is because the SPINPHARMA software only allows normalization along the direct dimension.

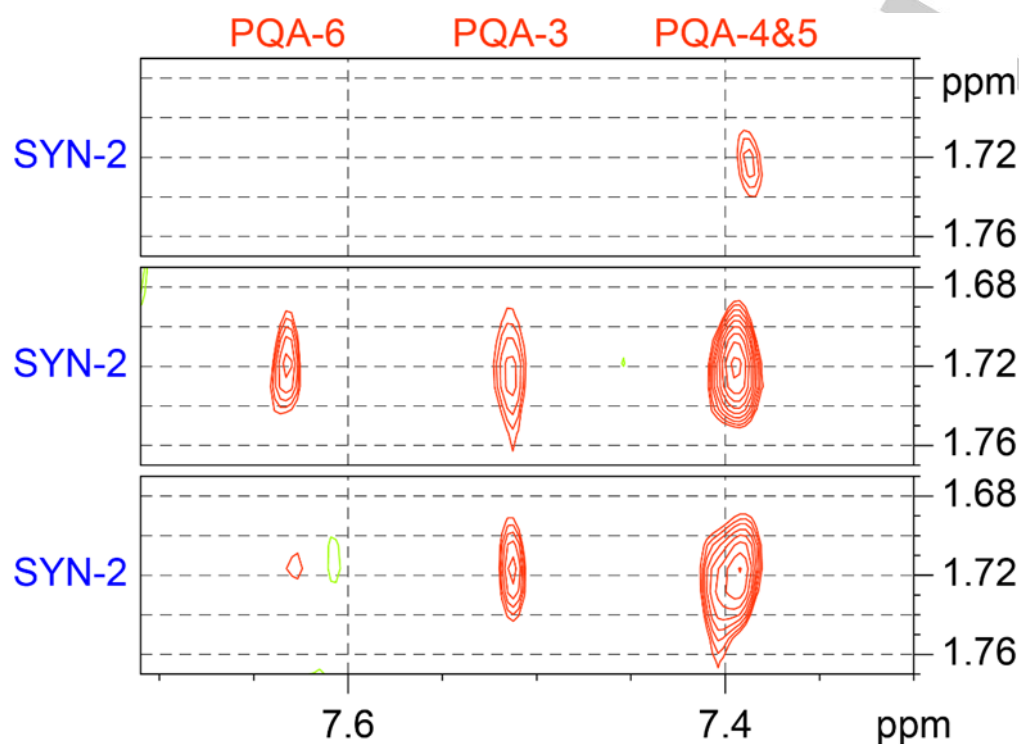**Detail of the NOESY spectra of PQA and SYN**

Figure S3: NOESY spectra showing cross peaks between SYN and PQA. Top panel with empty nanodiscs (ST1), middle panel with $A_{2A}R$ loaded nanodiscs (ST2) and bottom panel with with $A_{2A}R$ loaded nanodiscs in the presence of XAC (ST3). (PQA:SYN:XAC – 200:200:50 µM)

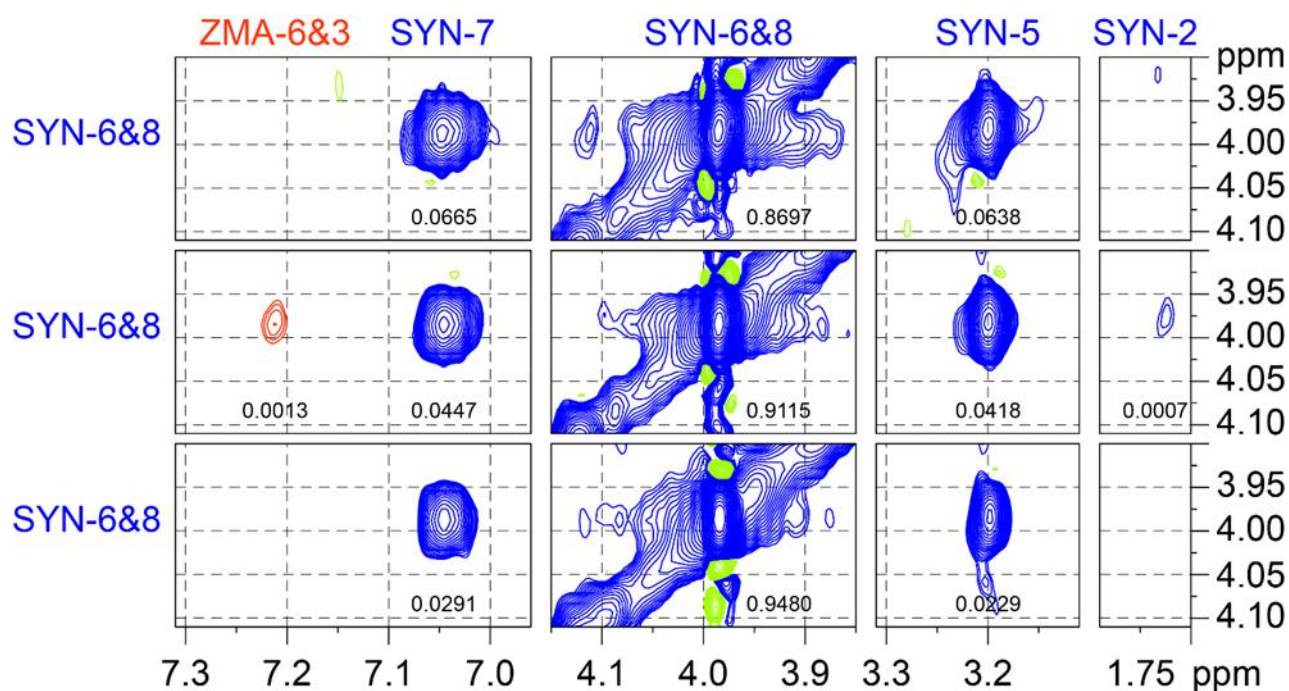**Detail of the NOESY spectra of ZMA and SYN**

Figure S4: NOESY spectra showing intraligand NOE's of SYN and one interligand NOE between SYN and ZMA. Top panel with empty nanodiscs (ST1), middle panel with $A_{2A}R$ loaded nanodiscs (ST2) and bottom panel with $A_{2A}R$ loaded nanodiscs in the presence of XAC (ST3). The numbers beneath the peaks indicate the corresponding normalized volumes. (ZMA:SYN:XAC – 200:200:50 µM)

Radioligand Binding

Cell membrane preparations

Sf9 insect cells recombinantly expressing human $A_{2A}R$ were broken using nitrogen cavitation and cells were collected by centrifugation at 100 000 x g for 60 min. The cell pellet was collected, resuspended and washed with 25 mM phosphate-buffered saline (PBS, pH 7.5, consisting of 100 mM NaCl in 100% D_2O) then centrifuged at 50 000 x g for 30 min; this was done three times. After washing, samples were frozen and stored at -80° C. Sf9 cell membrane preparations were washed three times with ice-cold 50 mM Tris- buffer at pH 7.4, then centrifuged at 48,000 g for 30 min each time to remove the NaCl in the storage buffer. After the last centrifugation step the obtained cell pellets were resuspended in 3 ml of 50 mM Tris-buffer at pH 7.4 and stored at -80° C. The protein content was determined by the Lowry method.[2] CHO cell membrane preparations recombinantly expressing the human $A_{2A}R$ (CHO-hA_{2A} or CHO-HA-hA_{2A}) were prepared as previously described.[3] For affinity measurement of eticlopride, L2 and SYN-115 human embryonic kidney (HEK) cell membranes recombinantly expressing human $A_{2A}Rs$ obtained from Perkin Elmer (HEK-hA_{2A}, Perkin Elmer, RBHA2AM400UA) were used.

Radioligand binding assays at human adenosine A_{2A} receptors

For radioligand binding assays the tritiated $A_{2A}R$-selective antagonist [³H]MSX-2 and the tritiated $A_{2A}R$-selective agonist [³H]CGS21680 were used.[3] The previously determined K_d-values of the employed radioligands at the human adenosine A_{2A} receptor are as follows: [³H]MSX-2, 7.29 nM; [³H]CGS21680, 25.0 nM.

Competition binding experiments with [³H]MSX-2 were performed in a final volume of 400 µl containing 4 µl of test compound dissolved in DMSO, 200 µL of buffer (50 mM Tris-buffer, pH 7.4), 100 µl of radioligand solution in the same buffer (final concentration 1 nM), and 100 µl of Sf9 insect cell membrane preparation expressing the human $A_{2A}R$ (50 µg protein per vial in 50 mM Tris-buffer containing 2 units (U)/ml of adenosine deaminase (ADA), or 100 µl of HEK cell membrane preparation expressing the human $A_{2A}R$ (8 µg protein per vial containing 2U/ml of ADA), or 100 µl of CHO cell membrane preparation expressing the human $A_{2A}R$ (50-100 µg protein per vial containing2U/ml ADA) respectively. ADA was added in order to convert adenosine present in the preparation to inosine since adenosine would otherwise interfere

with radioligand binding. Nonspecific binding was determined in the presence of the $A_{2A}R$ antagonist CGS15943 (final concentration 10 µM). Competition binding experiments with [³H]MSX-2 in the presence of 100 mM NaCl (final concentration) were performed in a final volume of 400 µl containing 4 µl of test compound dissolved in DMSO, 100 µL of buffer (50 mM Tris-buffer, pH 7.4), 100 µL of NaCl-containing buffer (400 mM NaCl, 50 mM Tris-buffer, pH 7.4), 100 µl of radioligand solution in 50 mM Tris-buffer (final concentration 1 nM), and 100 µl of Sf9 cell membrane preparation containing the human $A_{2A}R$ (50 µg protein per vial in 50 mM Tris-buffer). Nonspecific binding was determined in the presence of CGS15943 (final concentration 10 µM). After an incubation time of 30 min at rt, the assay mixture was filtered through GF/B glass fiber filters which were previously incubated in 0.3% polyethyleneimine (PEI) solution for 30 min using a Brandel cell harvester (Brandel, Gaithersburg, MD, USA). Filters were washed three times with ice-cold 50 mM Tris-HCl buffer, pH 7.4 (3-4 ml each). Then filters were transferred to scintillation vials, incubated for 9 h with 2.5 ml of scintillation cocktail (Luma Safe, Perkin Elmer), and counted in a liquid scintillation counter (Tri-Carb 2810 TR) with a counting efficiency of 52%. Three separate experiments were performed for determination of the IC_{50} values. Data were analyzed with the program GraphPad Prism, Version 4.1 (GraphPad Inc., La Jolla, CA).

Radioligand binding assays at human A_{2A} receptors reconstituted in nanodiscs

A preparation of human $A_{2A}R$ reconstituted in nanodiscs (250 µl in 25 mM phosphate-buffered saline (PBS), pH 7.5, consisting of 100 mM NaCl in 100% D_2O, 4.7 µM), was divided into 50 µl aliquots and stored at -80°C until use. For the assay pre-test the protein was diluted 1:2 with 50 mM Tris-buffer pH 7.4 and for further tests the protein aliquots were diluted 1:10 with 50 mM Tris-buffer pH 7.4. Competition binding experiments with [³H]MSX-2 were performed in a final volume of 400 µl containing 4 µl of test compound dissolved in DMSO, 200 µL buffer (50 mM Tris-buffer, pH 7.4), 100 µl of radioligand solution in the same buffer (final concentration 1 nM), and 100 µl of a suspension of human $A_{2A}R$ in nanodiscs. All other conditions were as described above for $A_{2A}R$ expressed in mammalian cells.

Agonists such as NECA and CGS21680 typically show a higher affinity for the receptor conformation that is labelled by an agonist radioligand (high affinity conformation for agonists) than for the conformation that is labelled by an antagonist radioligand. Therefore, the agonists NECA and CGS21680 display significantly higher affinity versus the agonist radioligand [³H]CGS21680 as compared to the antagonist radioligand [³H]MSX-2. In contrast, antagonists typically bind with identical (neutral agonists) or similar affinity (inverse agonists) to the receptor conformations labelled by agonist or antagonist radioligands.[4]

Table S3. Affinities of the agonists NECA and CGS21680 determined versus antagonist ([³H]MSX-2) and agonist ([³H]CGS21680) radioligands at human $A_{2A}R$ expressed in CHO-cells, or in Sf9 insect cells, respectively.

	K_i/K_D^* value ± SEM (nM)	
	NECA	**CGS21680**
Transfected CHO cells (human $A_{2A}R$)		
vs. [3H]MSX-2	**447** ± 148	**168** ± 36
vs. [3H]CGS21680	**35.1** ± 23.5	**25.0**± 11.4*
Transfected Sf9 insect cells (human $A_{2A}R$)		
vs. [3H]MSX-2	**167** ± 48[*]	**592** ± 21[***]
vs. [3H]CGS21680	**64.0** ± 9.8[ns]	**27.1** ± 6.8[ns]

[*]$p < 0.05$
[***]$p < 0.001$
 ns = not significant

Modulation of A_{2A} receptor binding by sodium ions

In the presence of NaCl (100 mM) the agonist curves (for NECA and CGS21680) determined at human $A_{2A}R$ expressed in Sf9 insect cells versus the antagonist radioligand [3H]MSX-2 were shifted to the right (Figure S4). The effect was more pronounced for NECA (6-fold shift) than for CGS21680 (2-fold shift) indicating that both agonists may prefer somewhat different receptor conformations. As expected, no NaCl shift was observed for CGS21680 versus the agonist radioligand [3H]CGS21680. These results clearly indicate that the $A_{2A}R$ expressed in Sf9 insect cells is functional.[5]
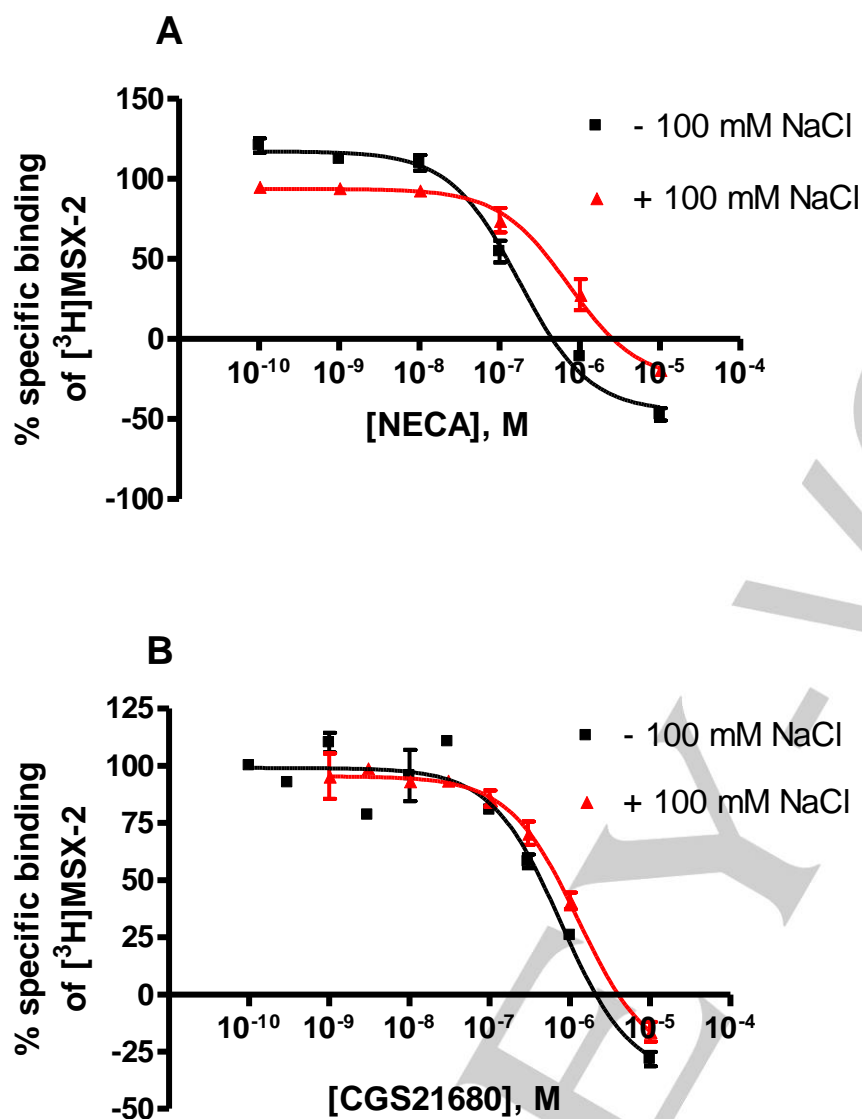
A

B

Figure S5. Competition binding experiments of the agonists (**A**) NECA, and (**B**) CGS21680 versus the A_{2A}-selective antagonist radioligand [3H]MSX-2 (1 nM) at human A_{2A} receptors expressed in Sf9 insect cells in the absence and in the presence of 100 mM NaCl.

(**A**) The calculated IC_{50}-values for NECA were **190** ± 55 nM (without NaCl) and **1160** ± 280 nM (in the presence of 100 mM NaCl, *$p < 0.05$, n = 3 ± SEM, 6-fold shift)

(**B**) The calculated IC_{50}-values for CGS21680 were **673** ± 24 nM (without NaCl) and **1440** ± 480 nM (in the presence of 100 mM NaCl, n = 3 ± SEM, 2-fold shift).
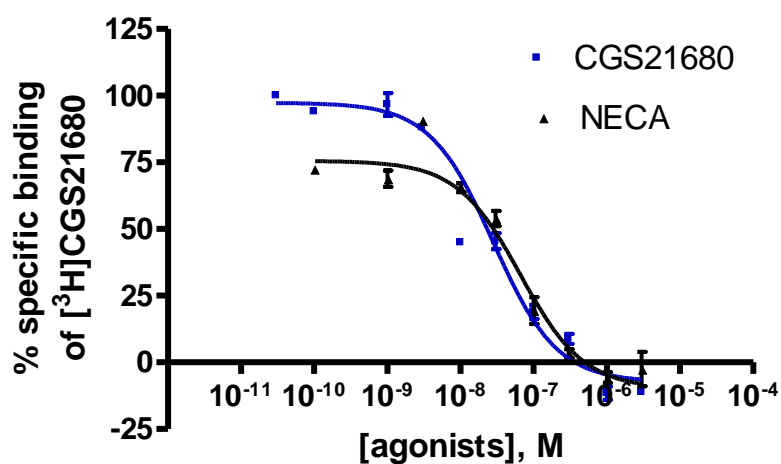
Figure S6. Competition binding experiments of the agonists NECA and CGS21680 versus the A_{2A}-selective agonist radioligand [³H]CGS21680 (5 nM) at human A_{2A} receptors expressed in Sf9 insect cells (n=3, performed in single points).
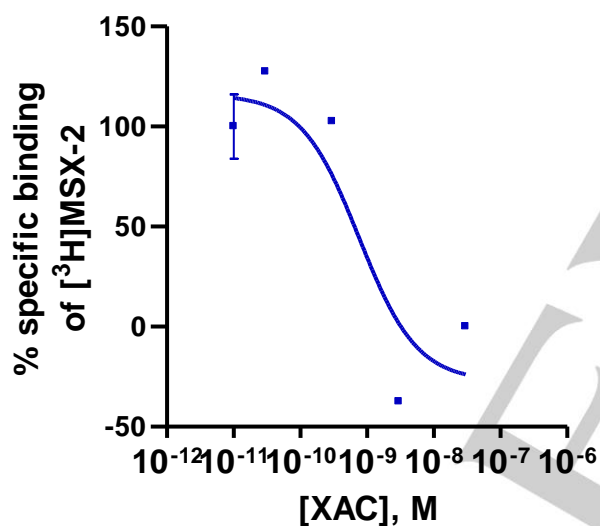

Figure S7. Competition binding experiment of the A_{2A}-antagonist XAC versus the A_{2A}-selective antagonist radioligand [³H]MSX-2 (1 nM) at human A_{2A}R reconstituted in nanodiscs. A single experiment was conducted and a K_i value for XAC of 0.650 nM was determined which is comparable with literature data.
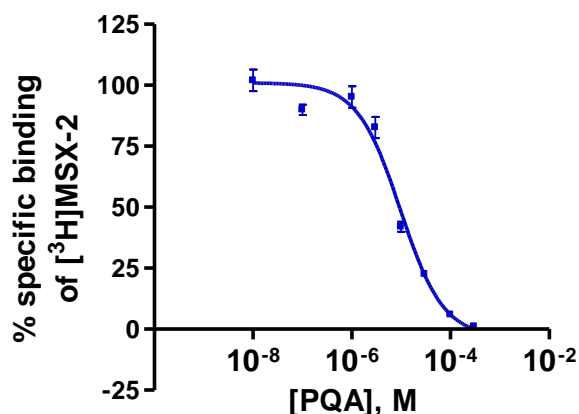
Figure S8: Competition binding experiment of PQA versus the $A_{2A}R$ antagonist radioligand [³H]MSX-2 at human $A_{2A}R$ expressed in HEK293 cells (n=3). For PQA a K_i value of 8.65 ± 0.79 µM was determined.
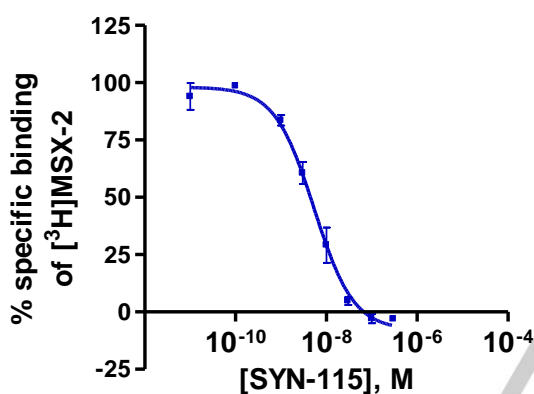

Figure S9: Competition binding experiment of SYN-115 versus the A_{2A} antagonist radioligand [³H]MSX-2 at human A_{2A} receptors expressed in HEK293 cells (n=3).A K_i value for SYN-115 of 5.17 ± 1.03 nM was determined.

Computational Methods

Generation of input structure for molecular dynamics simulations

Overall, 12 X-ray structures were downloaded from the Protein Data Bank,[6] (PDB entries 2YDO, 2YDV, 3EML, 3PWH, 3OAK, 3REY, 3RFM, 3UZA, 3UZC, 3VG9, 3VGA and 4EIY) and were used as starting points for the computational investigations. These structures represent different thermostabilized mutants of $A_{2A}R$ or chimera structures, in which $A_{2A}R$ is fused with another protein for easier crystallization. In addition some are partly co-crystallized with agonists and antagonists including the ligands ZMA, XAC and caffeine also used in this study. In order to make these structures comparable to the NMR measurements performed on the wild-type protein, the wild-type sequence was homology modelled taking the X-ray structures as templates one after another. Modeller 9.10,[7,8] was used with standard parameters and the flexible C-terminus and some amino acids from the N-terminus, for which no information was available, were removed. Missing loops, e.g. which were cut out to attach a second protein to form the chimera, were also modelled in this step. In this way, we ended up with 12 wild-type starting structures from Gly5 to Ala317. These were then placed into a homogeneous lipid bilayer using the Membrane Builder,[9] part of the CHARMM-GUI web service. Two preprocessing steps had to be performed before using the web interface. 1) The Orientations of Proteins in Membranes (OPM) database provides sets of coordinates for membrane proteins from the PDB, which are correctly aligned to the hydrocarbon core of the lipid bilayer to be used directly in the Membrane Builder. To generate the same orientation for our modelled wild-type structures, the generated homology models were aligned on the corresponding PDB structures provided by the OPM database using the

Molcad II program,[10] by minimizing the distance between Cα atoms. 2) Ligand structures were extracted from the PDB files, protonated by the software SPORES,[11] and stored as mol2-files to guarantee correct protonation and bonding states.

The following 5 STEPs were then performed using the interface: After upload of one of the wild-type structures to the web interface in PDB format, parameters for the protein and ligand were created (STEP 1). Disulfide bridges were created manually using the functionality of the web interface. To position the protein correctly in the membrane, the membrane was formed out of POPC molecules forming a rectangular unit cell and the minimal number of lipids around the protein in the x- and y-directions (the z-direction corresponds to the direction perpendicular to the membrane surface) was set to 2.0 (STEP 2). The water thickness was set to 25.0 Å. 0.15 M KCl was added representing physiological conditions (STEP 3). After preparing the different components first (STEP 4 of Membrane Builder) and assembling the components (STEP 5) including the energy minimization steps performed automatically by the Membrane Builder, the resulting files were downloaded without further equilibration of the system. The complete system provided as a PDB file by Membrane Builder was then used as input for the molecular dynamics simulations.

Molecular Dynamics Simulations

Molecular dynamics (MD) calculations were done with the AMBER 12 suite of programs.[12] Before starting these simulations, the residue names of the lipid molecules had to be translated into AMBER format using charmmlipid2amber.py. The protein and lipid parameters were taken from the modified version of the Cornell et al. force field,[13] (parm12SB) and from the AMBER lipid force field (lipid14),[14] respectively. The ligands were parameterized using the general AMBER force field (GAFF),[15] and AM1bcc charges using the ANTECHAMBER program.[16] After the LEAP program generated the parameter and coordinate files for the complete system including protein, ligand, lipids, ions and water molecules, the box dimensions were manually corrected to the values identified by Membrane Builder. In all simulations the particle mesh Ewald (PME) method was used to treat long-range electrostatic interactions and the SHAKE method,[17] to constrain bond lengths of bonds involving hydrogen atoms. The time step was set to 2 fs with a non-bonded cutoff of 10 Å.

All systems were first minimized by up to 20000 steps to account for differences in the AMBER and CHARMM force fields, since the latter was used in Membrane Builder for the lipid bilayer. The heating to 300 K was performed in two steps first from 0 to 100 K during 50 ps and then from 100 to 300 K during 1 ns of NVT-MD with harmonic restraints and with force constants of 10 kcal mol^{-1} Å^{-2} on the membrane, protein and ligand. To pre-equilibrate the membrane and relaxing the pressure to 1 bar, NPT-MD simulations were performed for 10 ns. The restraints on the protein and ligand were kept during this first equilibration step. Finally, the complete system was again equilibrated for another 10 ns slowly reducing the restraints on the protein and ligand. A production run of 100 ns followed and snapshots of the simulation were written out every 1 ps resulting in 100,000 complex structures for each of the 12 X-ray structures representing a thermodynamic ensemble available for further analysis.

Pose prediction of ligands without X-ray structure

For the ligands PQA and SYN, no X-ray structures are available up to now. Therefore, complex structures had to be proposed in order to be able to back-calculate INPHARMA spectra. Since exploring the complete conformational space to find the correct ligand pose is too time consuming using MD, faster but also more approximate methods were used to create first candidates of ligand poses. We used two different approaches: the docking program PLANTS,[18] and the alignment tool pharmacophore.[19] For both, the standard parameters were kept. PLANTS tries to fit the ligand into the active site of the protein by optimizing a score evaluating the steric fit, hydrogen bond and lipophilic interactions. Due to the flexibility of A₂ₐR, all 12 X-ray structure were used separately in this docking approach and the active site was defined by the corresponding ligands from which X-ray exist. PharmACOphore aligns one flexible ligand onto a fixed ligand by matching pharmacophoric features like ring systems and hydrogen bond acceptors and donors. The ligands XAC and ZMA were used as fixed ligands using the conformation seen in their X-ray structures in complex with the mutated forms of A₂ₐR as described above. PQA and SYN were aligned by optimizing the coordinates of the center of mass simultaneously to the torsion angles of single bonds. The resulting poses from both approaches were manually inspected. Since the protein adapts specifically to every ligand, PQA and SYN cannot be fit into the active site of smaller ligands by the docking tool or only show a limited number of favorable interactions. These structures were not considered further. Large steric overlaps were often seen for the poses proposed by pharmACOphore and these structures were also rejected. This selection

resulted in 3 PQA complex structures all resulting from the docking approach and 1 reasonable SYN structure from the pharmACOphore approach. For these remaining poses, the same MD protocol as described above was executed generating thermodynamic ensembles (again 100,000 snapshots were stored), which can then be validated by the agreement between the experimental and back-calculated spectra.

Comparison of experimental and back-calculated INPHARMA spectra

As described in Skjærven et al.,[20] a large number of complex structures should be used in the SpinPharma calculations to identify the correct poses. This is due to the fact that the back-calculated volumes of the INPHARMA peaks are very dependent on the proton-proton distances. In Onila et al.,[21] PLANTS was used to predict the ligand poses by optimizing a combination of the standard scoring function and a score describing the agreement of the experimental and theoretical spectra. Due to the large flexibility of the protein, this latter approach cannot be used here since the protein is kept rigid in the docking. Therefore, we follow another approach here: Due to the finite temperature and measuring time of the experiment, the experimental volumes don't result from a single structure but from the thermodynamic ensemble of structures. This ensemble would also be obtained, in the ideal case, by all the structures generated during a very long MD simulation. With such optimal ensembles for both ligands, we could back-calculate the volumes of the INPHARMA peak for each pair of complex structures and should be able to get the best agreement with the experiment by comparing the calculated volumes averaged over all complex structures taken from the MD simulation with the experimental ones. It is clear that the 100 ns simulations of this large and very flexible system are far from an exhaustive ensemble. Nevertheless, even the structures of the partial ensembles of the correct ligand poses should, on average, show better agreement with the experiment than all other possible poses. As a proof-of-concept, we took 400 complex structures for each ligand from the snapshots from the simulations (every 250 ps) and calculated the Pearson correlation coefficient between the experimental and back-calculated volumes of the INPHARMA signals for each pair of a ZMA and PQA complex structure resulting in 160 000 values. The back-calculated values were obtained with the SpInpharma program using the two-state model. The affinity value of ZMA were taken from literature,[22] and for PQA affinity were measured (Figure S6). The correlation time of the nanodiscs were calculated with Stoke's law using the following parameters; disc diameter: 9.6 nm,[23, 24] viscosity of deuterated water: 1.1 cP and a temperature of 298 K. An example input file is given in Figure S10.

```
# Input Files
Project_Directory               data/
Assignment_Ligand_1             PQA.asgn
Assignment_Ligand_2             ZMA.asgn
Experimental_Peak_List          exp_1.vols
# Relaxation Model Parameters
Spect_Frequency                 8e8
Correlation_Time_of_L1Free      0.10e-9
Correlation_Time_of_L2Free      0.10e-9
Correlation_Time_of_Complexes   124.0e-9
Cutoff                          5.0
# Kinetic Model Parameters
kinModel                        2
kL1                             16000
kL2                             87000000
# Concentrations
cL1_tot                         200
cL2_tot                         200
cT_tot                          4
```

Figure S10: Example input file for the SpInpharma calculation for PQA and ZMA based on structures taken from the MD simulations.

The resulting correlation coefficients for the best three docking structures of PQA are visualized as heat maps in Figure S11. For these calculations, the experimental values were generated using $A_{2A}R$ loaded disc volume integrals before and after XAC competition. To see changes occurring during the simulations, the values are arranged in a temporal order of the PQA and ZMA simulation in the x- and y-dimension, respectively. It can be clearly seen that the used ZMA structure has only a very weak influence on the correlation coefficient (vertical lines of very similar color). In contrast, significant changes can be seen between the different PQA simulations but also when comparing different time steps of the same simulation. Simulation 1 starts with correlation coefficients around 0 but these improve considerably during the first quarter of the simulation. Since the starting structure generated by docking or the pharmACOphore approach are very approximate, it is not unexpected that these show no agreement with the experiment. The MD simulation then optimizes the fit of the ligand into the binding site, which is verified by the improved correlation coefficient. The other two simulations show only very small changes over the course of the simulation. Simulation 3 even shows a worsening at the end of the simulation.

Overall, the pcc values are also slightly and significantly worse for simulation 2 and 3 compared to simulation 1, respectively. This can also be seen in the histograms of the correlation coefficients shown in Figure S12 and S13. To account for the fact that the simulation is not fully equilibrated at the start of the production run, i.e. large changes in the ligand structures are seen in the beginning of the simulation (see above), the histograms for only the last 60 ns of the simulations are given in the main document. If the empty disks are used as reference, the same result is obtained that simulation 1 gives on average the best correlation coefficients followed by simulation 2 (Figure S11). Simulation 3 again shows very bad correlation coefficients. Overall, the differences are, however, less pronounced as with the XAC titration reference. Additionally, the large improvement in simulation 1 cannot be seen with the empty nanodisc reference (data not shown).
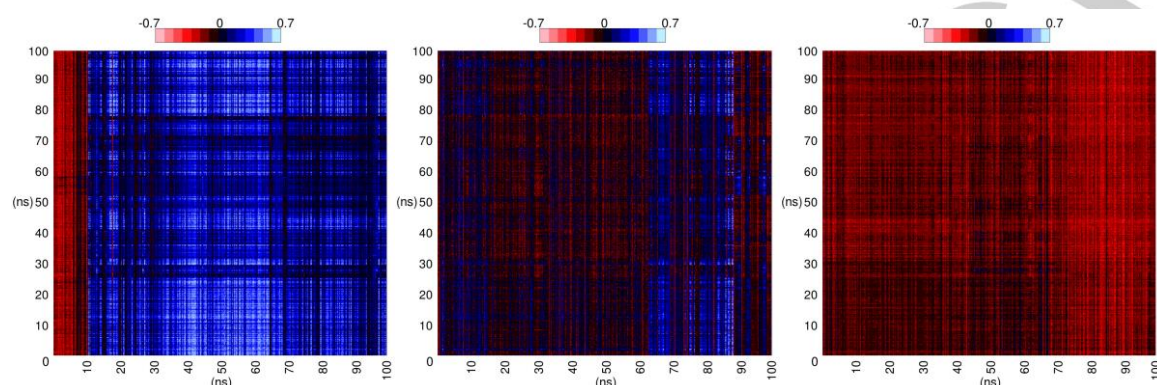

Figure S11: Heat map representing the Pearson correlation coefficients (PCC) comparing the experimental and back-calculated volumes of the INPHARMA signals. The values are arranged in a temporal order of the PQA and ZMA simulation in the x- and y-dimension, respectively. The three subfigures correspond to the three starting structures of PQA shown in the main document. (red) PCC = -1, (black) PCC = 0, (blue) PCC = 1
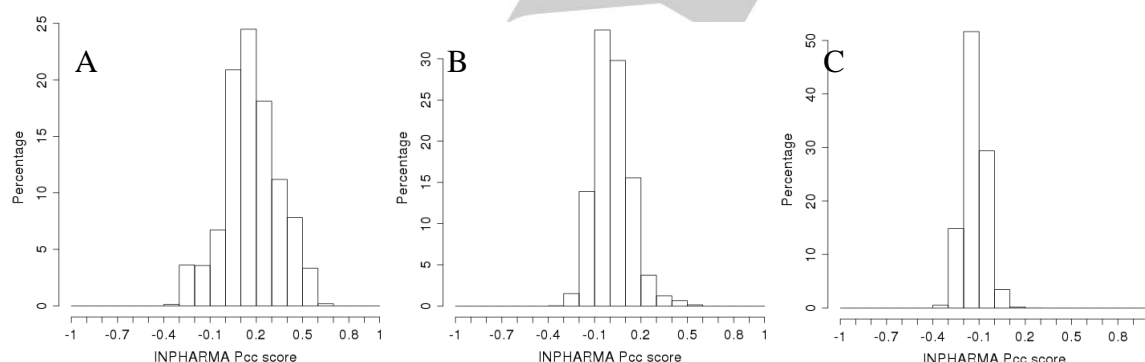

Figure S12: Histogram of Pearson correlation coefficients (PCC) comparing the experimental and back-calculated volumes of the INPHARMA signals of ZMA and PQA for the full 100 ns of the MD simulation without experiment restraints. The 160 000 calculated values are binned into intervals of 0.1 and the corresponding percentage of the total values calculated. A, B and C are based on the three different structures of PQA (see main text). The experimental values were taken from difference of the XAC titration.
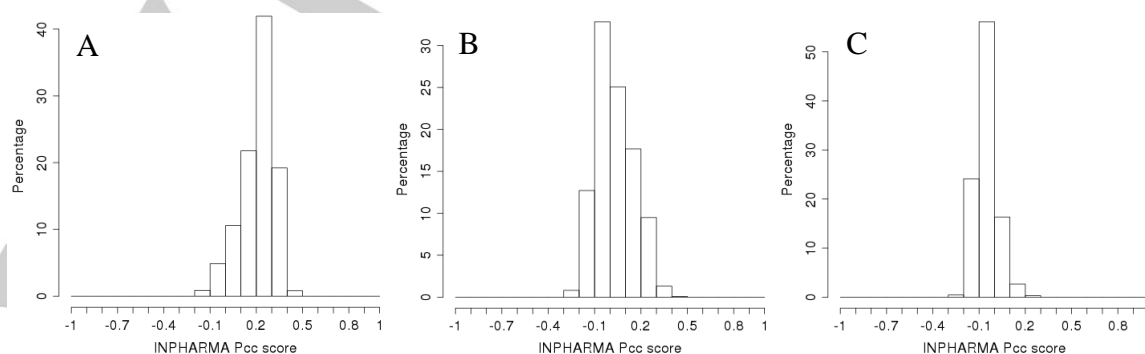

Figure S13: Histogram of Pearson correlation coefficients (PCC) comparing the experimental and back-calculated volumes of the INPHARMA signals of ZMA and PQA for the full 100 ns of the MD simulation without experiment restraints. The 160 000 calculated values

are binned into intervals of 0.1 and the corresponding percentage of the total values calculated. A, B and C are based on the three different structures of PQA (see main text). The experimental values were taken from the difference between empty and loaded discs.

References

[1] V. M. Sánchez-Pedregal, M. Reese, J. Meiler, M. J. Blommers, C. Griesinger, T. Carlomagno, *Angew Chem*. **2005**, *44*, 4172-5.

[2] O. H. Lowry, N. J. Rosebrough, A. L. Farr, R. J. Randall, *J. Biol. Chem.* **1951**, *193*, 265–275.

[3] C. E. Müller, J. Maurinsh, R. Sauer, *Eur J Pharm Sci.* **2000**, *10*, 259-65.

[4] K. Varani, S. Gessi, A. Dalpiaz, P. A. Borea, Br J Pharmacol. 1996, 117, 1693-701.

[5] H. Gutierrez-de-Teran, A. Massink, D. Rodriguez, W. Liu, G. W. Han, J. S. Joseph, I. Katritch, L. H. Heitman, L. Xia, A. P. Ijzerman, V. Cherezov, V. Katritch, R. C. Stevens *Structure* **2013**, *21*, 2175-85.

[6] H.M. Berman, J. Westbrook, Z. Feng, G. Gilliland, T.N. Bhat, H. Weissig, I.N. Shindyalov, P.E. Bourne, *Nucleic Acids Research* **2000**, *28*, 235-242. (www.rcsb.org)

[7] N. Eswar, M. A. Marti-Renom, B. Webb, M. S. Madhusudhan, D. Eramian, M. Shen, U. Pieper, A. Sali. *Current Protocols in Bioinformatics* **2006**, Supplement *15*, 5.6.1-5.6.30.

[8] B. Webb, A. Sali, *Methods Mol Biol*. **2014**, *1137*, 1-15

[9] S. Jo, T. Kim, W. Im, *PLoS ONE* **2007**, *2*, doi:10.1371/journal.pone.0000880

[10] M. Keil, R. J. Marhöfer, A. Rohwer, P. M. Selzer, J. Brickmann, O. Korb, T. E. Exner, *Frontiers in Bioscience* **2009**,*14*, 2559-2583.

[11] T. ten Brink, T. E. Exner, *J Chem Inf Model*. **2009**, *49*, 1535-46

[12] D.A. Case, R.M. Betz, W. Botello-Smith, D.S. Cerutti, T.E. Cheatham, III, T.A. Darden, R.E. Duke, T.J. Giese, H. Gohlke, A.W. Goetz, N. Homeyer, S. Izadi, P. Janowski, J. Kaus, A. Kovalenko, T.S. Lee, S. LeGrand, P. Li, C. Lin, T. Luchko, R. Luo, B. Madej, D. Mermelstein, K.M. Merz, G. Monard, H. Nguyen, H.T. Nguyen, I. Omelyan, A. Onufriev, D.R. Roe, A. Roitberg, C. Sagui, C.L. Simmerling, J. Swails, R.C. Walker, J. Wang, R.M. Wolf, X. Wu, L. Xiao, D.M. York and P.A. Kollman **2016**, AMBER 2016, University of California, San Francisco.

[13] T. E. Cheatham 3rd, P. Cieplak, P. A. Kollman, *J Biomol Struct Dyn.* **1999**, *16*, 845-62.

[14] C. J. Dickson, B. D. Madej, A. A. Skjevik, R. M. Betz, K. Teigen, I. R. Gould, R. C. Walker R., *J Chem Theory Comput.* **2014**, *10*, 865-879.

[15] J. Wang, R. M. Wolf, J. W. Caldwell, P. A. Kollman, D. A. Case, *J Comput Chem.* **2004**, *25*, 1157-74.

[16] J. Wang, W. Wang, P.A. Kollman, D.A. Case *J Mol Graph Model* **2006**, *25*, 247–260

[17] J-P. Ryckaert, G. Ciccotti, H. J. C. Berendsen, *Journal of Computational Physics* **1977**, *23*, 321-341.

[18] O. Korb, H. M. Möller, T. E. Exner, *ChemMedChem.* **2010**, *5*, 1001-6.

[19] O. Korb, P. Monecke, G Hessler, T. Stützle, T. E. Exner, *J Chem Inf Model*. **2010**, *50*, 1669-81.

[20] L. Skjærven, L. Codutti, A. Angelini, M. Grimaldi, D. Latek, P. Monecke, M. K. Dreyer, T. Carlomagno, *J Am Chem Soc.* **2013**, *135*, 5819-27.

[21] I. Onila, T. ten Brink, K. Fredriksson, L. Codutti, A. Mazur, C. Griesinger, T. Carlomagno, T. E. Exner, *J Chem Inf Model.* **2015**, *55*, 1962-72.

[22] C. E. Müller, K. A. Jacobson, *Biochim. Biophys. Acta* **2011**, *1808*, 1290–1308.

[23] I. G Denisov, Y. V. Grinkova, A. A. Lazarides, S. G. Sligar, *J Am Chem Soc.* **2004**, *126*, 3477-87.

[24] F. Hagn, M. Etzkorn, T. Raschle, G. Wagner, *J Am Chem Soc.* **2013**, *135*, 1919-25.

Author Contributions

Fredriksson K[1,2][*][#][+], Lottmann P[3][#], Hinz S[4], Onila I[1,2], Shymanets A[5], Harteneck C[5], Müller CE[4], Griesinger C[3], Exner TE[1,2][*]

1 Institute of Pharmacy, Eberhard Karls Universität Tübingen, Auf der Morgenstelle 8, 72076 Tübingen, Germany.

2 Department of Chemistry and Zukunftskolleg, Universität Konstanz, 78457 Konstanz, Germany.

3 Max Planck Institute for Biophysical Chemistry, Am Faßberg 11, 37077 Göttingen, Germany.

4 Universität Bonn, Pharma-Zentrum Bonn, Pharmazeutisches Institut, Pharmazeutische Chemie, An der Immenburg 4, 53121 Bonn, Germany.

5 Department of Pharmacology and Experimental Therapy, Institute of Experimental and Clinical Pharmacology and Toxicology, Interfaculty Center of Pharmacogenomics and Pharmaceutical Research (ICePhA), University of Tübingen, Tübingen, Germany.

* Corresponding Author(s) kai.fredriksson@tum.de and thomas.exner@uni-konstanz.de

# These authors contributed equally.

+ Present address: Fakultät für Chemie, Technische Universität München, Lichtenbergstraße 4, 85748 Garching, Germany.